Principle of Duality with Normalized Core Concept for Modeling Multi-Limb Transformers

Mohammad Shafieipour, Juan Carlos Garcia Alonso, Rohitha P. Jayasinghe, Aniruddha M. Gole

***Abstract*—The normalized core concept (NCC) was originally introduced for modeling of multi-limb transformers using the unified magnetic equivalent circuit. The NCC eliminates the need for information about the core dimensions, number of turns in the windings, and the core material. Therefore, incorporating NCC into a transformer modeling approach can significantly increase its usability in electromagnetic transient programs, as such information is usually only available to the transformer designer/manufacturer. In this paper, we show that the NCC is applicable to transformer models derived from the principle of duality, and as examples, three- and five-limb transformers are discussed. The resulting transformer models preserve the accuracy and numerical stability of duality-based models, while requiring only the information available in the nameplate and core aspect-ratios.**

***Keywords*—Multi-limb transformer modeling, principle of duality, normalized core concept (NCC), electromagnetic transient (EMT)-type program.**

I. Introduction

THE principle of duality is established as an efficient and numerically robust modeling tool that can properly represent the magnetic behavior of power transformers [1]. It has the advantage of being able to convert the physical magnetic circuit of an electromagnetic device, into its dual electric circuit counterpart, making it possible for electromagnetic transient (EMT)-type programs to adopt the resulting models, using standard circuit elements. Moreover, duality models can describe the distribution of magnetic flux in the core of virtually all transformer types, as they can be configured to match the topology of an arbitrary transformer. In other words, duality-based models are "topologically correct". The principle of duality was originally proposed for transformers by Cherry [2] and further developed by Slemon [3] to model non-linearities. In 2009 [4], a methodology based on mutually coupled inductors was introduced for representing terminal leakage measurements in the duality models for three-winding transformers; and it was later generalized for transformers with arbitrary number of windings [5]. Therefore, a systematic way of matching duality models with the leakage inductance measurements is available. However, determination of the magnetizing branch parameters for duality models consistent with an arbitrary core structure is difficult to achieve from measurement data. This is because standardized factory tests do not measure all the magnetizing parameters needed to construct the model. In the case of single-phase transformers, this difficulty may be overcome by assuming certain core geometry aspect-ratios and distributing the parameters accordingly for the given open-circuit test results [4], [6]. For multi-phase, multi-limb transformers, this difficulty is particularly highlighted, due to unavailability of standardized tests, limited transformer terminals, mutually coupled limbs, etc [4]. Therefore, when it comes to parameter determination of the magnetizing branches in duality-based models for multi-limb transformers, previous work [4], [7], [8], [9] has relied on detailed information about the core material (B-H curve or permeability μ), core dimension (cross-sectional area and effective length), and the number of turns in the windings. As a result, transformer manufacturers are called upon providing detailed information about their design, in the hope that accurate dual equivalent circuits can be determined. However, manufacturers are reluctant to provide such information. This has limited the use of multi-limbed duality-based models, despite the fact that in some EMT studies it is imperative to model the asymmetry of phase currents in such transformers. For example, it was shown in [10] (see Chapter 7) that a three-phase bank and a three-limb converter transformer, with comparable size and magnetizing current, can produce significantly different fault currents at different phases of the transformers. Neglecting such differences may lead to erroneous engineering decisions, such as transformer protection design, choice of insulating materials, power quality, etc.

In this paper we show that it is indeed possible to derive duality-based equivalent circuit models, based on typically available input parameters, by applying the normalized core concept (NCC) into duality-based equivalent circuits. The NCC was first introduced for unified magnetic equivalent circuit (UMEC) models [11], [12] and adopted by EMT-type software such as PSCAD/EMTDC [13]. The proposed technique, preserves the advantages of the duality models (i.e. accuracy, numerical stability, flexibility), while not requiring detailed information about the transformer inner design and material, nor the number of turns in the windings. Instead, it relies solely on the information available on the nameplate and on the factory acceptance test (FAT) report, plus the core aspect-ratios, similar to the approach used by the classical UMEC model. The proposed technique is applied to the conventional three- and five-limb (legged) transformer models. It is shown that the proposed technique accurately computes the internal parameter values. Excellent agreement

M. Shafieipour, J. C. Garcia A., and R. P. Jayasinghe are with Manitoba Hydro International Ltd., Winnipeg, Canada (e-mail of corresponding author: mshafieipour@mhi.ca, e-mail: jcgzipa@mhi.ca, jayas@mhi.ca).

A. M. Gole is with the Department of Electrical and Computer Engineering, University of Manitoba, Winnipeg, Canada (e-mail: Aniruddha.Gole@umanitoba.ca).

Paper submitted to the International Conference on Power Systems Transients (IPST2019) in Perpignan, France June 17-20, 2019.

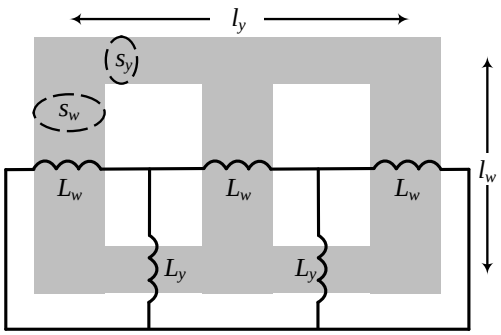

Fig. 1. Direct application of the principle of duality for the iron core of a three-limb transformer.

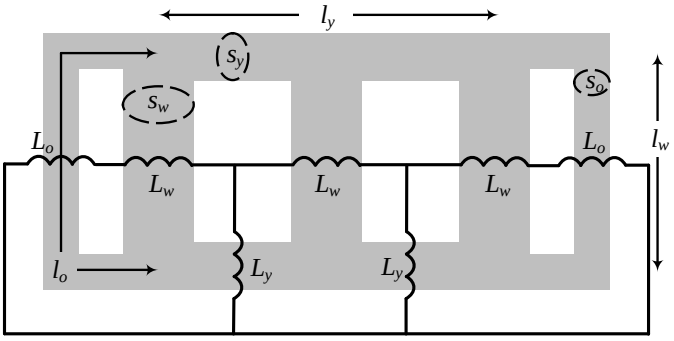

Fig. 2. Direct application of the principle of duality for the iron core of a five-limb transformer.

with an established EMT simulation model (UMEC) further validates the approach. In this paper for the sake of simplicity and brevity, linear circuit parameters are considered and non-linearity is left for future publications.

II. Limitation of Using Duality-Based Transformer Models

Dual models can be derived using two approaches [1]: 1) the classical method that derives electric circuits from magnetic circuits [2], and 2) direct application of the principle of duality by placing electric components on the geometry of the transformer [3]. If the same assumptions are made, both techniques will produce the exact same results; however, the second approach is simple to apply, especially in more complex transformer windings-core configurations. In this paper we use the second approach.

Fig. 1 is the direct application of the principle of duality to a three-limb transformer core. From this figure, it is realized that the magnetizing branches are purely inductive. Incorporation of core losses is trivial and is achieved via parallel linear resistances as done in [4], [14]. For the purpose of this paper, the inductances are set to be linear. Non-linear inductive branches (saturation, deep saturation and hysteresis) will be covered in subsequent publications. The following expression explains the linear behavior of the winding-limb and yoke inductances L_w, L_y [3]

$$L_w = \frac{N^2 \cdot \mu \cdot s_w}{l_w}, \quad L_y = \frac{N^2 \cdot \mu \cdot s_y}{l_y} \tag{1}$$

where N is the number of turns of the energized winding and μ is the permeability of the core. In (1), the cross-sectional areas of the yoke s_y and winding-limb s_w, as well as the effective lengths of the yoke l_y and winding-limb l_w are according to Fig. 1. Despite simplicity of (1), in most cases, none of the needed information to compute (1) is available to system designers, as the transformer manufacturers do not release such data. This poses a practical challenge when using duality-based model of a three-limb transformer.

Similar difficulty arises when attempting to derive duality-based model for a five-limb transformer as in Fig. 2. For this case, in addition to (1), a similar expression can be written for the outer-limb

$$L_o = \frac{N^2 \cdot \mu \cdot s_o}{l_o}. \tag{2}$$

Again, information for computing the magnetizing branches (inductors in Fig. 2) using (1) and (2) is usually not available to system designers, rendering the use of such model practically limited.

III. The Proposed Methodology: Normalized Core Concept Applied to the Principle of Duality

A. Preliminaries

In the proposed technique, the NCC is applied to the principle of duality. Therefore, it requires the same input parameters as the classical UMEC model [11], [12] for determining parameters of the magnetizing branches. To facilitate further discussion, these input parameters are reviewed below.

1) Magnetizing Current: The magnetizing current I_m can be obtained from

$$I_m = \sqrt{I_\Phi^2 - I_c^2} \tag{3}$$

where I_Φ is the excitation current and I_c is the core eddy current loss. These parameters are typically available in the FAT report. As mentioned earlier, the magnetizing branches in this paper are assumed to be purely inductive (i.e. $I_c = 0$). This reduces (3) to

$$I_m = I_\Phi \tag{4}$$

resulting in a simpler subsequent discussion. Generalization with (3) is straightforward.

2) Core Aspect-Ratios: The core aspect-ratios defined for a three-limb transformer (Fig. 1) are defined based on the yoke and winding-limb dimensions [11], [12]

$$r_s = \frac{s_y}{s_w}, \quad r_l = \frac{l_y}{l_w}. \tag{5}$$

As shown in Fig. 2, a five-limb transformer has yokes and winding-limbs, as well as outer-limbs. Therefore, for the five-limb case, in addition to (5), the following core aspect-ratios are also defined [12]

$$r'_s = \frac{s_y}{s_o}, \quad r'_l = \frac{l_y}{l_o}. \tag{6}$$

While the ratios in (5) and (6) are not found in the nameplate, commercial EMT-type software [13] has already used them for transformer modeling and it is expected that good estimates of these parameters can be provided by transformer or

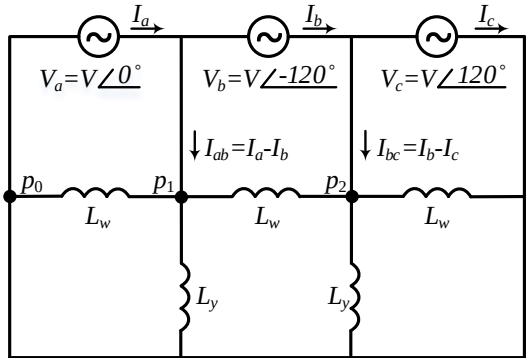

Fig. 3. Duality-derived equivalent circuit of a three-limb transformer during the excitation current measurement. Typically in the FAT report only one value of $I_m = (|I_a| + |I_b| + |I_c|)/3$ is recorded.

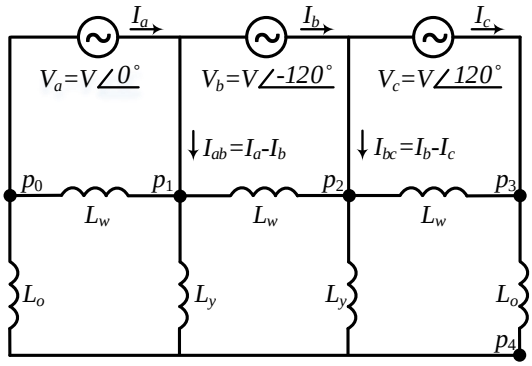

Fig. 4. Duality-derived equivalent circuit of a five-limb transformer during the excitation current measurement. Typically in the FAT report only one value of $I_m = (|I_a| + |I_b| + |I_c|)/3$ is recorded.

system engineers. It is worth mentioning that the maximum error caused by inaccurate core aspect-ratios in NCC can analytically be derived, a subject that is left for future work.

B. Duality-Derived Equivalent Circuit Parameters Based on the NCC

During the measurement of the excitation current, regardless of the total number of windings in a transformer, one winding is energized and the rest of the windings are left open. Therefore, the circuit shown in Fig. 3 can properly represent the three-limb transformer (Fig. 1) during such measurements. This is despite the fact that it does not posses any electrical component (inductor) to model the leakage reactances. This is true as the leakage inductances are only defined or measured when more than one winding is present in the circuit [4], [1]; a condition that is not met at the time of excitation current measurements. Similarly for the five-limb case, the open-circuit test performed at the time of excitation current measurement, is not affected by the leakage inductances and thus the open-circuit test equivalent circuit for the model of Fig. 2 is as shown in Fig. 4. Therefore, for both three- and five-limb cases, the magnetizing current (4) can be represented as follows:

$$I_m = \frac{|I_a| + |I_b| + |I_c|}{3} \tag{7}$$

where I_a, I_b, and I_c are the phase currents as shown in Figs. 3 and 4.

In order to define components of the above mentioned duality-based equivalent circuits based on the NCC, we first use (1) to write

$$\frac{L_y}{L_w} = (\frac{s_y}{s_w})(\frac{l_y}{l_w})^{-1}. \tag{8}$$

Using (8) and (5) we can express ratio of the yoke inductance L_y over the winding-limb inductance L_w as

$$\frac{L_y}{L_w} = \frac{r_s}{r_l} \tag{9}$$

which can be written as

$$Y_y = Y_w \cdot \frac{r_l}{r_s} \tag{10}$$

where Y_w and Y_y are purely-susceptant admittances corresponding to the winding-limb and yoke, respectively. They can be obtained from the following expressions

$$Y_w = \frac{1}{j\omega L_w}, \quad Y_y = \frac{1}{j\omega L_y} \tag{11}$$

where $\omega = 2\pi f$ is the angular frequency.

The relationships shown in (7) to (11) are applicable to both three- and five-limb cases. Similar expressions for the outer-limb can also be defined applicable to only five-limb models. To do that, we use (1) and (2) to write

$$\frac{L_y}{L_w} \cdot \frac{L_o}{L_y} = (\frac{s_y}{s_w})(\frac{l_y}{l_w})^{-1} \cdot (\frac{s_y}{s_o})^{-1}(\frac{l_y}{l_o}) \tag{12}$$

Using (5) and (6), it can be written as

$$\frac{L_o}{L_w} = \frac{r_s}{r_l} \cdot \frac{r'_l}{r'_s} \tag{13}$$

which in terms of admittance values is

$$Y_o = Y_w \cdot (\frac{r_l}{r_s} \cdot \frac{r'_s}{r'_l}) \tag{14}$$

with the admittance Y_o defined similar to (11) as

$$Y_o = \frac{1}{j\omega L_o}. \tag{15}$$

In the proposed technique, the unknown parameters are defined based on the impedance associated with the winding-limb admittance Y_w. Therefore it is given a concise name

$$\alpha = \frac{1}{Y_w} = j\omega L_w \tag{16}$$

to facilitate shorter notations. If we multiply both sides of (7) by α/I_m we get

$$\alpha = \frac{\alpha(|I_a| + |I_b| + |I_c|)}{3I_m}. \tag{17}$$

Since α represents a physical impedance value (16) it must be positive. Therefore, α can be distributed into the magnitude signs on the right-hand side (RHS) and thus we have

$$\alpha = \frac{|\alpha I_a| + |\alpha I_b| + |\alpha I_c|}{3I_m}. \tag{18}$$

In the sequel, procedures for determining the value of α and subsequently computing all magnetizing branch parameters for three- and five-limb transformer models are introduced using the relationships presented above.

1) The Three-Limb Case: From Fig. 3, it is seen that

$$I_{ab} = I_a - I_b, \quad I_{bc} = I_b - I_c. \tag{19}$$

Furthermore, it is well-understood that by having a balanced voltage source with no zero-sequence component, the sum of the fluxes and their corresponding magneto-motive forces (MMFs) generated by the three phases must be equal to zero. Therefore, by knowing that the principle of duality converts MMF into current, the sum of phase currents has to be zero

$$I_a + I_b + I_c = 0. \tag{20}$$

The relationship in (20) can also be proven using electric circuit analysis as shown in the Appendix. Using (19) and (20) the following system of linear algebraic equations is obtained

$$\begin{bmatrix} I_a \\ I_b \\ I_c \end{bmatrix} = \begin{bmatrix} 1 & -1 & 0 \\ 0 & 1 & -1 \\ 1 & 1 & 1 \end{bmatrix}^{-1} \cdot \begin{bmatrix} I_{ab} \\ I_{bc} \\ 0 \end{bmatrix}. \tag{21}$$

Using the nodal analysis in Fig. 3 where p_0 is taken as the reference point and the Kirchhoff's current law (KCL) is applied at nodes p_1 and p_2, the node-voltage equations have the following matrix form

$$\begin{bmatrix} I_{ab} \\ I_{bc} \end{bmatrix} = \begin{bmatrix} 2Y_w + Y_y & -Y_w \\ -Y_w & 2Y_w + Y_y \end{bmatrix} \cdot \begin{bmatrix} V_a \\ -V_c \end{bmatrix}. \tag{22}$$

If we multiply both sides of (22) by α in (16) and use (10) we can write

$$\begin{bmatrix} \alpha I_{ab} \\ \alpha I_{bc} \end{bmatrix} = \begin{bmatrix} 2 + \frac{r_l}{r_s} & -1 \\ -1 & 2 + \frac{r_l}{r_s} \end{bmatrix} \cdot \begin{bmatrix} V_a \\ -V_c \end{bmatrix}. \tag{23}$$

Since all variables on the RHS of (23) are known, the values of αI_{ab} and αI_{bc} can be obtained. Further, we multiply (21) by α and re-write it as

$$\begin{bmatrix} \alpha I_a \\ \alpha I_b \\ \alpha I_c \end{bmatrix} = \begin{bmatrix} 1 & -1 & 0 \\ 0 & 1 & -1 \\ 1 & 1 & 1 \end{bmatrix}^{-1} \cdot \begin{bmatrix} \alpha I_{ab} \\ \alpha I_{bc} \\ 0 \end{bmatrix} \tag{24}$$

which can be solved analytically using the already available αI_{ab} and αI_{bc}. Therefore, values of αI_a, αI_b, and αI_c can be determined. Now that all elements on the RHS of (18) are available for the three-limb core, α can be computed. Subsequently, (16) along with (10) and (11) are used to evaluate the sought-after L_w and L_y.

The values of L_w and L_y computed as explained above, will be identical to that of (1), eliminating the need for core dimensions, permeability of the core material, and the number of turns in the energized winding. Instead, only the core aspect-ratios and the magnetizing current are required for the proposed computations. It is important to note that for the magnetizing current, only the average of the RMS currents on the three phases (I_m as in (7)) is used, without relying on the values of the phase currents separately. This is consistent with typical FAT reports where only the average is registered (see Figs. 3 and 4).

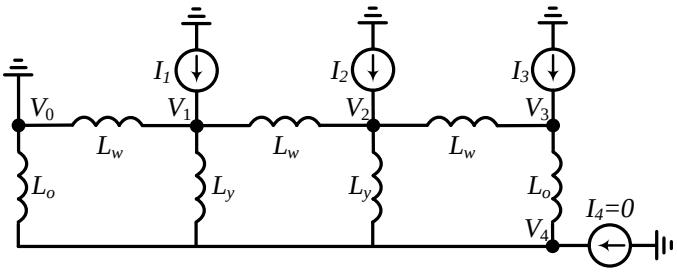

Fig. 5. Circuit of Fig. 4 represented using independent current sources. No voltage source is connected to p_4 in Fig. 4, thus $I_4 = 0$.

2) The Five-Limb Case: In order to derive values of L_w, L_y, and L_o for a five-limb transformer based on the NCC, we define an equivalent circuit for Fig. 4, in terms of independent current sources as shown in Fig. 5 and apply KCL to form the following system

$$\begin{bmatrix} I_1 \\ I_2 \\ I_3 \\ I_4 \end{bmatrix} = \begin{bmatrix} \mathtt{a} & -Y_w & 0 & -Y_y \\ -Y_w & \mathtt{a} & -Y_w & -Y_y \\ 0 & -Y_w & \mathtt{b} & -Y_o \\ -Y_y & -Y_y & -Y_o & \mathtt{c} \end{bmatrix} \cdot \begin{bmatrix} V_1 \\ V_2 \\ V_3 \\ V_4 \end{bmatrix} \tag{25}$$

where

$$\mathtt{a} = 2Y_w + Y_y, \quad \mathtt{b} = Y_w + Y_o, \quad \mathtt{c} = 2(Y_y + Y_o). \tag{26}$$

In Fig. 5, V_i is the voltage appearing at node p_i of Fig. 4 where p_0 is taken as the reference point ($V_0 = 0$). By looking at the independent voltage sources in Fig. 4 which are connected in series, it is easy to see that

$$V_1 = V_a, \quad V_2 = V_a + V_b = -V_c, \quad V_3 = V_a + V_b + V_c = 0 \tag{27}$$

and by comparing Figs. 4 and 5 one can realize that

$$I_1 = I_{ab}, \quad I_2 = I_{bc}, \quad I_3 = I_c. \tag{28}$$

However, the current source injecting I_4 into the circuit of Fig. 5 does not have a physical representation as no source is directly connected to p_4 in Fig. 4. Thus as shown in Fig. 5 we have

$$I_4 = 0. \tag{29}$$

Knowing that for the five-limb case both (10) and (14) are applicable, we multiply (25) by α defined in (16) and use (27), (28) and (29) to get

$$\begin{bmatrix} \alpha I_{ab} \\ \alpha I_{bc} \\ \alpha I_c \\ 0 \end{bmatrix} = \begin{bmatrix} \mathtt{d} & -1 & 0 & -\frac{r_l}{r_s} \\ -1 & \mathtt{d} & -1 & -\frac{r_l}{r_s} \\ 0 & -1 & \mathtt{e} & -\frac{r_l}{r_s} \cdot \frac{r'_s}{r'_l} \\ -\frac{r_l}{r_s} & -\frac{r_l}{r_s} & -\frac{r_l}{r_s} \cdot \frac{r'_s}{r'_l} & \mathtt{f} \end{bmatrix} \cdot \begin{bmatrix} V_a \\ -V_c \\ 0 \\ V_4 \end{bmatrix} \tag{30}$$

where

$$\mathtt{d} = 2 + \frac{r_l}{r_s}, \quad \mathtt{e} = 1 + \frac{r_l}{r_s} \cdot \frac{r'_s}{r'_l}, \quad \mathtt{f} = 2(\frac{r_l}{r_s})(1 + \frac{r'_s}{r'_l}). \tag{31}$$

Values of all parameters on the RHS of (30) are available except for V_4. Since the 4th element of the left-hand side is zero, Kron reduction [15] is applicable by solving for V_4 to obtain a (3×3) system. As a result, it becomes possible to

Model	r_s	r_l	r'_s	r'_l	L_w^{entered}(H)	L_y^{entered}(H)	L_o^{entered}(H)	I_m^{recorded}(mA)	L_w^{computed}(H)	L_y^{computed}(H)	L_o^{computed}(H)
Three-Limb	1	2.4	-	-	1.2	0.5	-	7.7399746	1.2000012	0.5000005	-
Five-limb	1	1.9	1.1	2.1	2.66	1.4	2.6727272	2.1863597	2.6600015	1.4000007	2.6727287

TABLE I

THE ENTERED (KNOWN) PARAMETERS WITH THEIR COMPUTED COUNTERPARTS USING THE PROPOSED TECHNIQUE FOR THREE-LIMB (FIG. 3) AND FIVE-LIMB (FIG. 4) DUALITY-BASED MODELS. PINK AND BLUE COLUMNS REPRESENT KNOWN AND COMPUTED VALUES, RESPECTIVELY.

compute αI_{ab}, αI_{bc}, and αI_c. Subsequently, αI_a and αI_b are available as

$$\alpha I_b = \alpha I_{bc} + \alpha I_c, \quad \alpha I_a = \alpha I_{ab} + \alpha I_b. \tag{32}$$

Therefore, the value of α can be determined for the five-limb core using (18). Subsequently, inductances L_w, L_y, and L_o of Fig. 4 (and Fig. 2) are computed via (16), (14), (10), (11), and (15). This completes the numerical determination of the magnetizing branch parameters for a five-limb duality-based model using the magnetizing current and core aspect-ratios without the need to have detailed information about the transformer's inner design.

IV. NUMERICAL RESULTS

A. Method Validation

In order to numerically validate the analytical expressions presented in Section III, the circuits of Figs. 3 and 4 are created in EMT software [13] with assumed (known) magnetizing branch parameters as shown in Table I (pink columns). The AC sources have a voltage magnitude of $V = 1.32$V where the frequency is 60Hz. The corresponding excitation currents are recorded when the systems reach the steady-state condition. The resulting magnetizing currents are then used in the proposed technique to compute the magnetizing branch parameters (blue-shaded columns in Table I). In all cases, highly accurate results are observed. Note that in the table, the difference between the entered and the computed values are dictated by the voltage source internal resistance that is set to $R_0 = 10^{-6}\Omega$ for all sources (see Fig. 9).

B. Comparison with the UMEC Model

The UMEC model has been shown to produce accurate results when compared with measurement results [11], [12], [10]. Therefore, in this paper we use UMEC as a reference solution in the EMT studies. For that purpose, the circuit of Fig. 6 is created in EMT-type program (PSCAD) [13] for both three- and five-limb cases. In order to be consistent with the linear assumption made in this paper, the UMEC-model's saturation is disabled. As shown in Fig. 6, the open circuit test is achieved by energizing one side and separating the other side from the ground with 1MΩ resistors[1]. For the three-limb case, the transformer detailed in Table 7.1 of [10] is examined. The size of the transformer is 187.5MVA with $f = 50$Hz and the voltage at the energized winding is 16kV (line-to-line). The core aspect-ratios are $r_s = 1$ and $r_l = 0.7409$. The excitation current[2] is $I_\Phi = 0.6059\%$ of the rated current. It

[1]To ensure numerical stability in EMT simulations, it is generally advised to avoid "hanging nodes" by placing a large resistance between the open nodes and the reference node (ground).

[2]The UMEC model implemented in PSCAD asks for the magnetizing current. In the simulations, this parameter is adjusted to read the expected average excitation current.

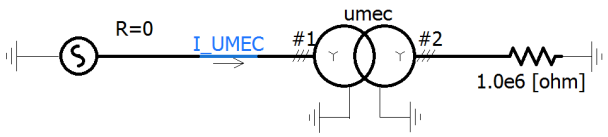

Fig. 6. The UMEC model under open-circuit test in EMT software [13].

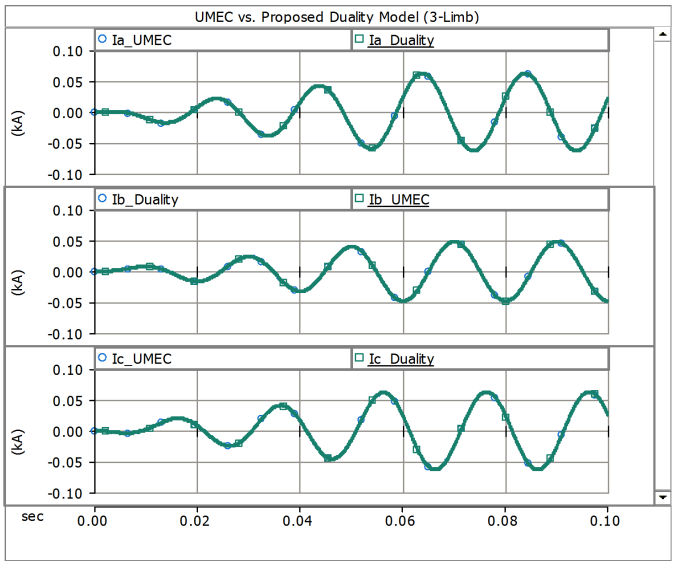

Fig. 7. Comparing the excitation phase currents produced by the UMEC and proposed models for a three-limb 187.5MVA transformer studied in [10].

is computed from the RMS magnitudes of $|I_a| = 0.043$kA, $|I_b| = 0.037$kA, and $|I_c| = 0.043$kA reported in Section 7.1.1 of [10]. For the five-limb case, the transformer of [12] is considered (see Table 1 therein). It is a 61MVA transformer operating at 50Hz with the energized winding rated at 11kV. The reported core aspect-ratios are $r_s = 0.683$, $r_l = 1.08$, $r'_s = 1.74$, and $r'_l = 0.836$. From the magnetizing current peaks (0.083kA, 0.08kA, 0.083kA), the excitation current is evaluated as $I_\Phi = 1.811\%$. Figs. 7 and 8 compare time-domain simulation results of the phase currents recorded at the source terminals (I_a, I_b, I_c) of the UMEC (Fig. 6) and the proposed duality models (Figs. 3 and 4) for the three- and five-limb cases, respectively. Essentially identical results are observed for all three phase currents, both in three- and five-limb cases. This demonstrates the numerical validity of the proposed technique when used in EMT simulations.

V. CONCLUSIONS

This paper introduces a technique for incorporating the NCC into multi-limb duality-based transformer models. The introduced model, is a duality transformer model which only requires nameplate data and core aspect-ratios. For the linear

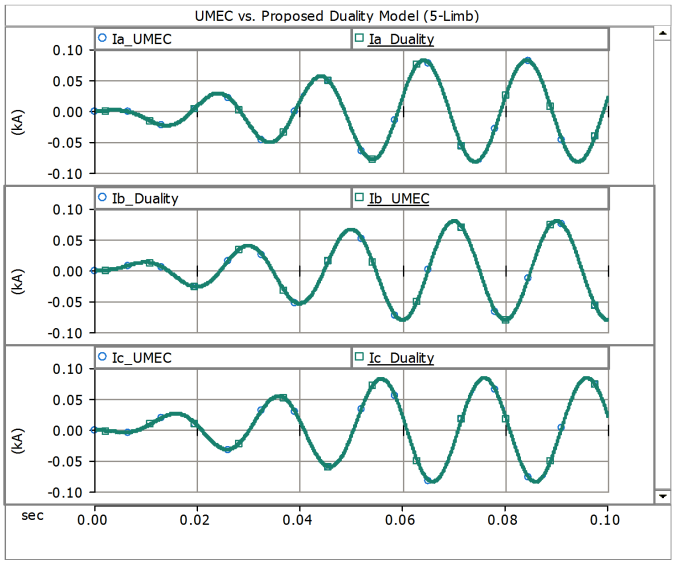

Fig. 8. Comparing the excitation phase currents produced by the UMEC and proposed models for a five-limb 61MVA transformer studied in [12].

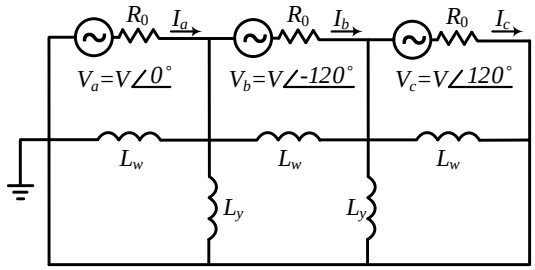

Fig. 9. The circuit of Fig. 3 with the source internal series resistances present.

models discussed in this paper, results agree to machine precision with the well-established UMEC model. In future work, non-linear magnetizing branches will be introduced to the proposed technique. Such duality-based transformer modeling approach would be a suitable candidate for use in EMT-type programs as it requires typically available input parameters, while being able to model hysteresis and saturation phenomena with the numerical robustness and accuracy of duality-based transformer models.

APPENDIX

In order to prove (20), we generalize the circuit of Fig. 3 to the circuit shown in Fig. 9 where AC sources constitute small internal series resistance of $R_0 \rightarrow 0\ \Omega$. By letting $Z_1 = j\omega L_w, Z_2 = j\omega L_y$, and $Z_3 = Z_1||Z_2$, we can form the mesh loops depicted in Fig. 10. Note that I_a, I_b, and I_c are the same in Figs. 9 and 10. The loop equations are

$$\begin{aligned} R_0 I_a + Z_3(I_a - I_d) &= V_a \\ R_0 I_b + Z_1(I_b - I_d) &= V_b \\ R_0 I_c + Z_3(I_c - I_d) &= V_c \\ Z_3(I_d - I_a) + Z_1(I_d - I_b) + Z_3(I_d - I_c) &= 0. \end{aligned} \tag{33}$$

Adding all equations in (33) and knowing that $V_a + V_b + V_c = 0$, we get

$$R_0(I_a + I_b + I_c) = 0. \tag{34}$$

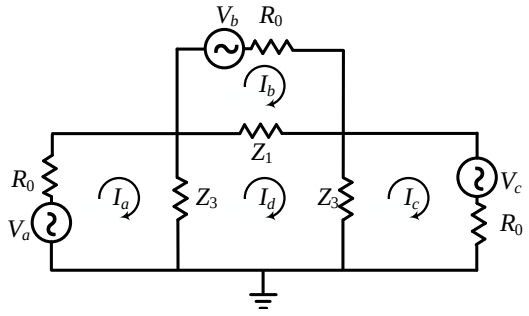

Fig. 10. The circuit of Fig. 9 re-arranged with equivalent impedances forming the desired mesh loops.

The internal series resistance of the AC sources R_0 is small but can not practically be exactly zero due to non-zero physical copper losses. Numerical EMT simulation [13] of Fig. 9 with $R_0 = 0$ would also render numerical instability. Therefore the only viable solution to (34) is (20). This completes the proof.

REFERENCES

[1] S. Jazebi *et al*., "Duality Derived Transformer Models for Low-Frequency Electromagnetic Transients - Part I: Topological Models," *IEEE Trans. Power Del.*, vol. 31, no. 5, pp. 2410–2419, Oct. 2016.

[2] E. C. Cherry, "The duality between interlinked electric and magnetic circuits and the formation of transformer equivalent circuits," in *Proc. Phys. Soc.*, Feb. 1949, vol. B, no. 62, pp. 101-111.

[3] G. R. Slemon, *Elect. Mach. Drives*. Reading MA, USA: Addison-Wesley, 1992.

[4] F. de Leon, and J. A. Martinez, "Dual Three-Winding Transformer Equivalent Circuit Matching Leakage Measurements," *IEEE Trans. Power Del.*, vol. 24, no. 1, pp. 160–168, Jan. 2009.

[5] C. Alvarez-Marino, F. de Leon and X. M. Lopez-Fernandez, "Equivalent Circuit for the Leakage Inductance of Multiwinding Transformers: Unification of Terminal and Duality Models," *IEEE Trans. Power Del.*, vol. 27, no. 1, pp. 353–361, Jan. 2012.

[6] S. Jazebi, F. de Leon, A. Farazmand and D. Deswal, "Dual Reversible Transformer Model for the Calculation of Low-Frequency Transients," *IEEE Trans. Power Del.*, vol. 28, no. 4, pp. 2509–2517, Oct. 2013.

[7] Xusheng Chen, "A three-phase multi-legged transformer model in ATP using the directly-formed inverse inductance matrix," *IEEE Trans. Power Del.*, vol. 11, no. 3, pp. 1554–1562, Jul. 1996.

[8] J. A. Martinez, R. Walling, B. A. Mork, J. Martin-Arnedo and D. Durbak, "Parameter determination for modeling system transients-Part III: Transformers," *IEEE Trans. Power Del.*, vol. 20, no. 3, pp. 2051–2062, Jul. 2005.

[9] Q. Wu, S. Jazebi, and F. de Leon, "Parameter Estimation of Three-Phase Transformer Models for Low-Frequency Transient Studies from Terminal Measurements," *IEEE Trans. Magn.*, vol. 53, no. 7, pp. 1–8, Jul. 2017.

[10] Wade G. Enright, "Transformer models for electromagnetic transient studies with particular reference to HVdc transmission", Ph.D. dissertation, Dept. Electrical and Electronic Eng., Univ. Canterbury, Christchurch, New Zealand, 1669. [Online]. Available: https://ir.canterbury.ac.nz/handle/10092/3279

[11] W. Enright, O. B. Nayak, G. D. Irwin, and J. Arrillaga, "An electromagnetic transients model of multi-limb transformers using normalized core concept," *Proc. Int. Conf. Power Syst. Transients,* Seattle, USA, (Jun. 22–26) (1997) 93–98.

[12] W. G. Enright, O. Nayak, and N. R. Watson, "Three-phase Five-Limb Unified Magnetic Equivalent Circuit Transformer Models for PSCAD V3," *Proc. Int. Conf. Power Syst. Transients,* Budapest, Hungary, (Jun. 20–24) (1999) 462-467.

[13] Manitoba Hydro International Ltd. (Feb. 6, 2019), *PSCAD/EMTDC,* [Online]. Available: https://hvdc.ca/pscad/

[14] S. Jazebi and F. de Leon, "Experimentally Validated Reversible Single-Phase Multiwinding Transformer Model for the Accurate Calculation of Low-Frequency Transients," *IEEE Trans. Power Del.*, vol. 30, no. 1, pp. 193–201, Feb. 2015.

[15] G. Kron, *Tensor Analysis of Networks*. John Wiley and Sons, 1965.